Electrochimica Acta 233 (2017) 256–261

Contents lists available at ScienceDirect

Electrochimica Acta

journal homepage: www.elsevier.com/locate/electacta

Influence of probe size for local electrochemical impedance measurements

Caio Palumbo de Abreu[a,b], Camila Molena de Assis[a,c], Patricia H. Suegama[d], Isolda Costa[b], Michel Keddam[a], Hercilio G. de Melo[c], Vincent Vivier[a,*]

[a] Sorbonne Universités, UPMC Univ Paris 06, CNRS, Laboratoire Interfaces et Systèmes Electrochimiques, 4 place Jussieu, F-75005, Paris, France
[b] Instituto de Pesquisas Energéticas e Nucleares, IPEN/CNEN-SP, Av. Prof. Lineu Prestes, 2242, CEP 05508-000, São Paulo, SP, Brazil
[c] Departamento de Engenharia Metalúrgica e de Materiais, Escola Politécnica, Universidade de São Paulo, CP 61548, Zip Code 05424-970, São Paulo, SP, Brazil
[d] Faculdade de Ciências Exatas e Tecnologia–UFGD, Rodovia Dourados–Itahum, km 12, CP 364, Zip Code 79.804-970, Dourados, MS, Brazil

ARTICLE INFO

Article history:
Received 23 December 2016
Received in revised form 27 February 2017
Accepted 3 March 2017
Available online 6 March 2017

Keywords:
Local electrochemical impedance spectroscopy
Local current density
Microelectrodes
Probe size
Stray capacitance

ABSTRACT

Local electrochemical impedance spectroscopy (LEIS) is a promising technique for the characterization of heterogeneous surface reactivity. Significant development of LEIS relies on the improvement of the spatial resolution for reaching the micrometer scale. This work presents the influence of the probe size, especially in the high frequency domain where an inductive-like response ascribed to the stray dielectric capacitance between the two electrodes of the probe used for performing the local current measurement can be observed. A detailed analysis of the whole set-up (electrode geometry and measuring device) allows an analytical expression of the impedance for the whole system to be obtained. Based on the analysis of this expression and on experimental results, two different strategies have been proposed to cancel the HF time constant: a post treatment of the results via a preliminary electrical characterization of the local probe or the minimization of the electrolyte resistance by measuring the local potential in the close vicinity of the substrate. Both approaches were shown to be efficient.

1. Introduction

The characterization of the local reactivity of an electrified interface is usually performed with the use of local probes with an adequate size depending on the spatial resolution required, but also on the technique used. The scanning electrochemical microscopy (SECM) is by far the most widely used local technique in electrochemistry [1–3], but only few works have been performed in the frequency domain. For instance, the use of a single frequency measurements at an ultra-microelectrode (UME) allows to map the surface heterogeneity [4–7], whereas the use of the ac-SECM in substrate generation–tip collection mode allows a complex collection efficiency to be obtained, and thus to study the formation and the relaxation of reaction intermediates involved in complex mechanisms such as proton reduction [8,9] or iron oxidation [10]. On the other hand, local current-density can be measured using the scanning vibrating electrode technique (SVET) [11–13] without the requirement of adding any redox mediator in solution. This technique then gives rise to the local electrochemical impedance spectroscopy (LEIS) as an alternative route for the local investigation of an electrochemical reaction, which has been developed in the 90's with the pioneering works of Isaacs *et al.* [14,15]. It consists in using two reference electrodes (*e.g.* a bi-microelectrode) that are positioned close to the interface of interest for measuring the local current density in solution from the potential difference between the two micro-reference electrodes immersed in the electrolyte. The current is thus measured as the ohmic drop between the two sensing electrodes in solution, and depends on both the electrode distance and the electrolyte conductivity. Thus, the local impedance can be calculated similarly to a usual (*i.e.* global) electrochemical impedance using a frequency response analyzer, that is as the ratio of the potential to the local current density for each frequency [14]. This technique was successfully used for the investigation of coating degradation [16–18], pitting corrosion of iron chromium alloy [19,20], magnesium alloy corrosion [21], or time-constant distribution of a passive film formed on a stainless steel sample [22]. However, one of the key-points for the technique is the spatial resolution that is governed by the probe size and the probe-to-sample distance. Indeed, for many applications such as coating degradation [16,18], a spatial resolution in the millimeter range is usually sufficient, but

* Corresponding author.
E-mail address: vincent.vivier@upmc.fr (V. Vivier).

http://dx.doi.org/10.1016/j.electacta.2017.03.017
0013-4686/

for other applications such as the mapping of surface reactivity that depends on the grain size [21] or for the characterization of a single pit [19], a spatial resolution of few tens of micrometers is required. This can be obtained by diminishing both the size of each wire used for sensing the local potential in solution and the distance between these two wires. In this work, a specific attention has been paid to the response of local probes of few tens micrometers, since in the high frequency domain, a capacitive coupling may exist between two adjacent micro-wires, whereas in the low frequency domain, the potential difference to be measured between these two probes can be very small. A detailed analysis of experimental results was thus provided for a model system involving redox mediators studied at a metallic electrode, thus allowing the separation of the electrochemical contribution from the stray contribution of the measurement setup.

2. Experimental

All the electrochemical measurements were performed using a home-made setup previously described [21,23] and presented in Fig. 1. It consisted in a potentiostat with which the global impedance was measured allowing the surface averaged value of the electrode response to be recorded, whereas simultaneously, the local potential and the local current density were probed in solution with a bi-microelectrode [14,24,25]. Data acquisitions were performed using a 4-channel frequency response analyzer (1254–Solartron) allowing multiple transfer functions to be measured simultaneously. The probe positioning was achieved with stepper motors (UTM25, Newport) driven by a motion encoder (MM4005, Newport) allowing a spatial resolution of 0.2 μm in the three directions. A homemade DC-offset coupled with a variable gain differential amplifier was used for the measurement of the local potential difference in solution (*vide infra*). With such a configuration, it was possible to measure a potential difference of *ca* 1 μV between the two probes in the low frequency domain ($f < 100$ mHz). Interestingly, this limit can be lowered by adapting the amplification stages before and after the DC-offset as a function of the local impedance to be measured. The distance between the probe and the substrate was controlled by slowly bringing the probe in contact with the substrate and then by withdrawing it to the desired distance. This allowed a vertical positioning with a resolution of ±5 μm, which was estimated with an independent set of experiments.

The working electrode was a platinum rod of 0.5 cm in diameter laterally insulated by a cataphoretic paint (200 V/2 minutes, then cured for 1 hour at 80 °C) and an epoxy-resin (Radiospare), thus

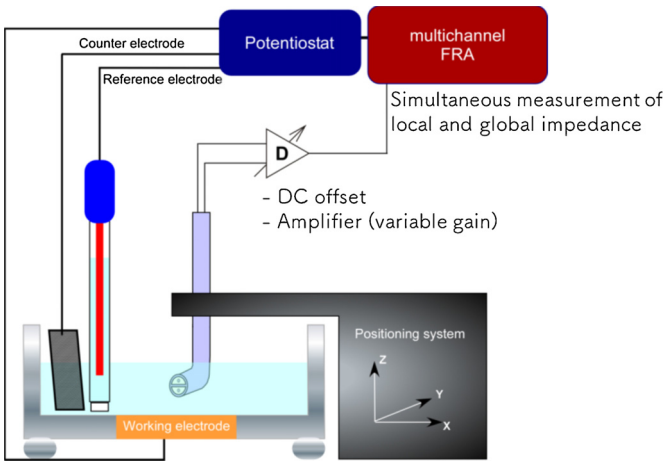

Fig. 1. Sketch of the experimental setup.

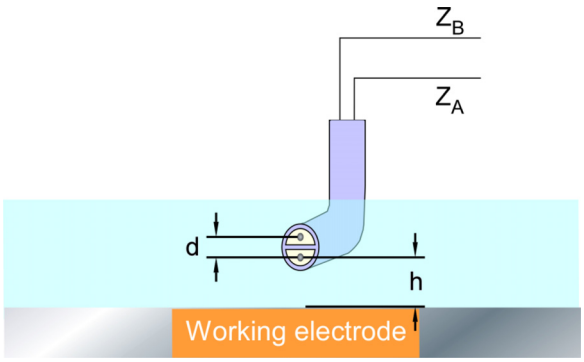

Fig. 2. Sketch of local probe with the relevant parameters investigated in this work.

exposing a disk of 0.2 cm^2 surface area to the electrolyte. No specific activation of the electrode has been performed before the experiments. The counter electrode was a platinum gauze of large surface area surrounding the whole electrochemical cell in order to minimize the frequency dispersion due to the geometry of the system, and the reference electrode was a saturated calomel electrode (E/SCE = E/NHE - 0.244 V, where NHE is the normal hydrogen electrode).

The local probe used for performing local impedance measurements consisted in a bi-microelectrode prepared with silver microwires laterally insulated with a cataphoretic paint (200 V/1 minute, then cured for 1 hour at 80 °C) and sealed with an epoxy-resin in a capillary. The apex of the probe was polished and each of the wires was anodized in a chloride containing solution to obtain an Ag/AgCl reference electrode. This procedure is in marked contrast to the use of platinum probes since it allows to minimize the contribution of the Nernst potential due to redox species in solution [26].

The spatial resolution that can be reached with such a probe depends on the size of the microwires, the distance between the two microwire centers (d), and the distance between the probe and the substrate (h) as sketched in Fig. 2. In addition, even if nanoelectrodes are available, the use of probe smaller that 1 mm is still challenging with respect to the potential measurement to be performed [27]. In this work, local impedance measurements were performed either by measuring the local current with the local probe and the global potential, or by measuring the local current with the local probe and the local potential with the closest probe to the electrode surface, similarly to the definition of Bayet *et al.* [28], emphasized later on by Huang *et al.* [27]. It is interesting to mention that the former experiment corresponds to the local impedance that can be usually measured with commercial equipment and will be labelled as local impedance in the following, whereas for the second definition, a home-made equipment is required and will be labelled local interfacial impedance [27].

Some electrical impedance measurements were performed with a dielectric interface (Solatron 1296A) coupled to a frequency response analyzer (Solartron 1255) for the characterization of the probes.

All electrolytic solutions (10 mM ferri/ferrocyanide + 0.5 M KCl) were prepared with analytical grade chemicals in twice distilled water.

3. Results and discussion

Fig. 3a shows the global impedance diagram in a Nyquist representation obtained with a 5 mm in diameter platinum electrode for the ferri/ferrocyanide redox couple (10 mM) in 0.5 M KCl electrolytic solution. The EIS response is typical of a redox system in solution. It shows the electrolyte resistance as the high

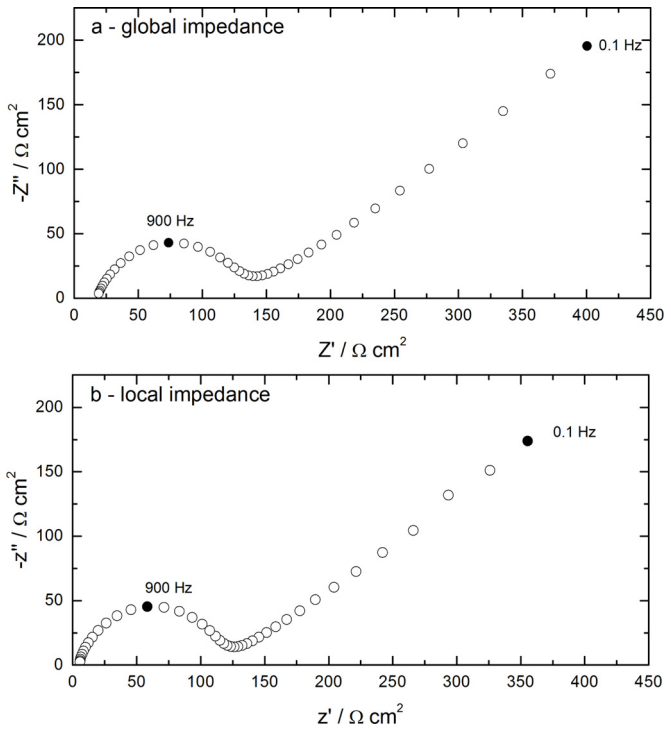

Fig. 3. EIS and LEIS diagrams recorded simultaneously in a ferri/ferrocyanide (10 mM) + 0.5 M KCl electrolyte at the equilibrium potential (E = 0.195 V/SCE). The distance between the two wires and the radius of each wire were 150 μm; probe-to-sample distance h = 100 μm.

frequency limit, a capacitive loop ascribed to the charge transfer resistance in parallel with the double layer capacitance (with a characteristic frequency of about 900 Hz), and the Warburg impedance corresponding to the diffusion of the electroactive species. Interestingly, the local impedance response presented in Fig. 3b and measured above the Pt electrode center with a bi-electrode (each Ag/AgCl microelectrode was 150 μm in diameter and the distance between the two wires was 150 μm) shows the same behavior for the impedance response of the system, with the same time-constants and a similar amplitude. It should however be mentioned that the electrolyte resistance may be different from one experiment to another, since, for local measurement, it depends not only on the electrolyte conductivity, but also on the probe to substrate distance. In addition, Ferrari et al. showed that the global impedance response is not affected by the probe position above the electrode [29]. Indeed, it was shown that whatever the probe position (close to the electrode center, or close to the electrode edge), that is, at locations where the local current densities are different, the global impedance response remains unchanged for both the amplitude of the different contributions and the time-constant. Therefore, any screening of the global current-potential distribution by the probe may be disregarded.

The low frequency limit is usually difficult to measure with good accuracy. This is due to the fact that for most electrochemical systems, the magnitude of the low frequency impedance is larger than the high frequency contribution, in other words, the ac current to be measured decreases with the frequency. In the literature, this problem is often circumvented by decreasing the electrolyte concentration (*i.e.* by working in low conductive medium to optimize the resolution) [30]. However, such a choice strongly modifies the electrochemical system properties and results in difficulties for comparison with literature data. Indeed, the main drawback for the measurement is the dc-potential difference that exists between the two probes used to sense the local potential, which can however be corrected using a level shifter to improve the accuracy of the measurement, that is by adjusting the dc potential offset to 0 mV with a preliminary experiment performed in the same electrolyte [31]. It should also be mentioned that the use of a scanning vibrating electrode technique (SVET) provides another way to discard the residual dc-potential contribution that always exists between two different electrodes [28,32]. Thus, the use of an intermediate low gain amplifier to initially correct the dc offset allows to work in concentrated electrolyte as it was done in this work (0.5 M KCl solution).

The same local experiment was performed with a smaller probe, namely, two Ag/AgCl microelectrodes of 20 μm in diameter each, separated by a distance of about 15 μm (Fig. 4). The LEIS responses are similar with either a large or a small probe except in the high frequency domain for which an inductive behavior is observed when the distance between the two Ag/AgCl wires is decreased. This kind of response is usually encountered in the case of studies on large batteries because of the stray impedance (*i.e.* inductance) of the wires used for measuring the very low impedance systems, but this hypothesis must be ruled out in the case of localized impedance since the measured quantities are in the ohm range or larger.

In fact, this effect can be understood by modelling more precisely how the ac potential actually measured between the two electrodes depends on their own electrochemical impedances, the inter-electrode dielectric capacitance and the resistance of the potential source in solution. Let us consider the electrical sketch of the setup used for performing the measurement (Fig. 5). It consisted in a differential amplifier, the two inputs of which are connected to the Ag/AgCl microreference electrodes. The short distance between the two wires gives rise to a stray capacitance, C_p, whereas the impedance of each probe is Z_A and Z_B. The local potential difference, $\Delta V_{probe} = V_B - V_A$, measured between the two probes allows the local current density, j_{loc}, to be readily calculated as

$$j_{loc} = \frac{\Delta V_{probe}}{\rho\, d} \tag{1}$$

where ρ is the electrolyte conductivity and d the distance between the two probes. This quantity corresponds to the actual

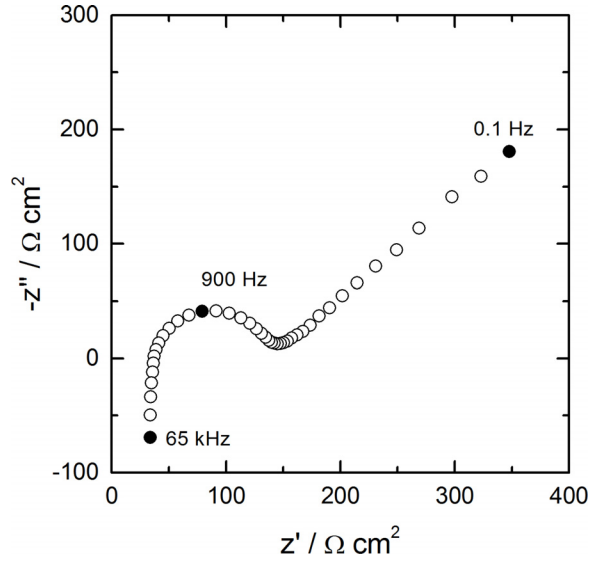

Fig. 4. LEIS diagrams measured with a small probe (diameter of each wire: 20 μm; distance between wires: 15 μm; probe-to-sample distance h = 100 μm) in a ferri/ferrocyanide (10 mM) + 0.5 M KCl electrolytic solution at the equilibrium potential.

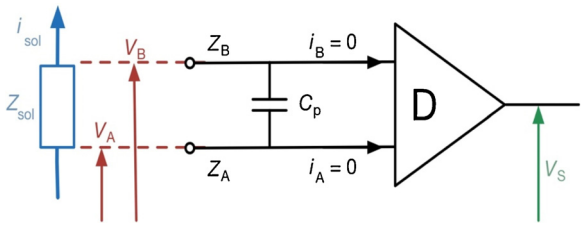

Fig. 5. Electrical circuit describing the local current amplification set-up from the measurement of the local potential difference between two probes.

local current density flowing in the solution and sensed by the microprobe at a distance h of the interface. Assuming an ideal behavior of the differential amplifier, that is, infinite input impedance, infinite open-circuit gain and flat band-pass, only the impedance of the individual microelectrodes and the stray capacitance have to be taken into account as parasitic effects in the measurement of the local current density. The current, i_c, flowing in the capacitance can thus be expressed as

$$i_c = \frac{j_{loc}\rho d}{Z_A + \frac{1}{j\omega C_p} + Z_B} \tag{2}$$

and the potential difference, ΔV_{diff}, between the two inputs of the differential amplifier is given by

$$\Delta V_{diff} = \frac{i_c}{j\omega C_p} = \frac{j_{loc}\rho d}{j\omega C_p (Z_A + Z_B) + 1} \tag{3}$$

The stray capacitance can be independently determined by measuring the impedance of the microreference electrodes in air, as shown in Fig. 6. A capacitive behavior was obtained with a low frequency limit in the range of GΩ, and a capacitance of about 7 pF from the fit of the experimental results with a Voigt element. It should be mentioned that this value was not obtained with a usual potentiostat but with a dielectric interface, which allows such a low value to be measured.

Moreover, the stray capacitance also depends on the distance between the two wires as usually observed for the patterns of printed circuit boards measured in the high frequency range [33]. Additionally, when the experiment is performed in an electrolytic solution, similar impedance diagrams were obtained but with a larger stray capacitance (between 25 to 100 pF), the value of which depends on the electrolyte conductivity. This was ascribed to the additional capacitive contribution introduced by the ac current path connecting the two microprobes through the surrounding electrolyte.

Similarly, the impedance of each microelectrode was obtained by measuring independently their electrochemical impedance in the electrolyte at the equilibrium potential, *i.e.* when no current flows between the two electrodes (data not presented), which shows that the impedance of each probe can be expressed as

$$Z_A = R_1 + \frac{R_2}{1 + j\omega R_2 C} \tag{4}$$

R_2 and C (the capacitance of the electrode immersed in solution, that is the combination of the double layer capacitance and that of the thin AgCl layer at the Ag microelectrode surface) depend only on the probe geometry, whereas R_1 depends on the distance between the two microwires. As the two probes used for measuring the local current density are assumed to be identical, $Z_A = Z_B$ and Eq. 3 can be rewritten as

$$\Delta V_{diff} = \frac{i_c}{j\omega C_p} = \frac{j_{loc}\rho d}{j\omega C_p 2\left(R_1 + \frac{R_2}{1+j\omega R_2 C}\right) + 1} \tag{5}$$

Thus, the local current density can be obtained from

$$j_{loc} = \frac{\Delta V_{diff}}{\rho d}\left(j\omega C_p 2\left(R_1 + \frac{R_2}{1 + j\omega R_2 C}\right) + 1\right) \tag{6}$$

and the local impedance measured by the experimental setup, $z_{measured}$, is expressed as

$$z_{measured} = \frac{\Delta V_{applied}}{j_{loc}} = \frac{\Delta V_{applied}}{\frac{\Delta V_{diff}}{\rho d}\left(j\omega C_p 2\left(R_1 + \frac{R_2}{1+j\omega R_2 C}\right) + 1\right)} \tag{7}$$

where $\Delta V_{applied}$ is the applied potential between the substrate and the reference electrode. Thus the local impedance

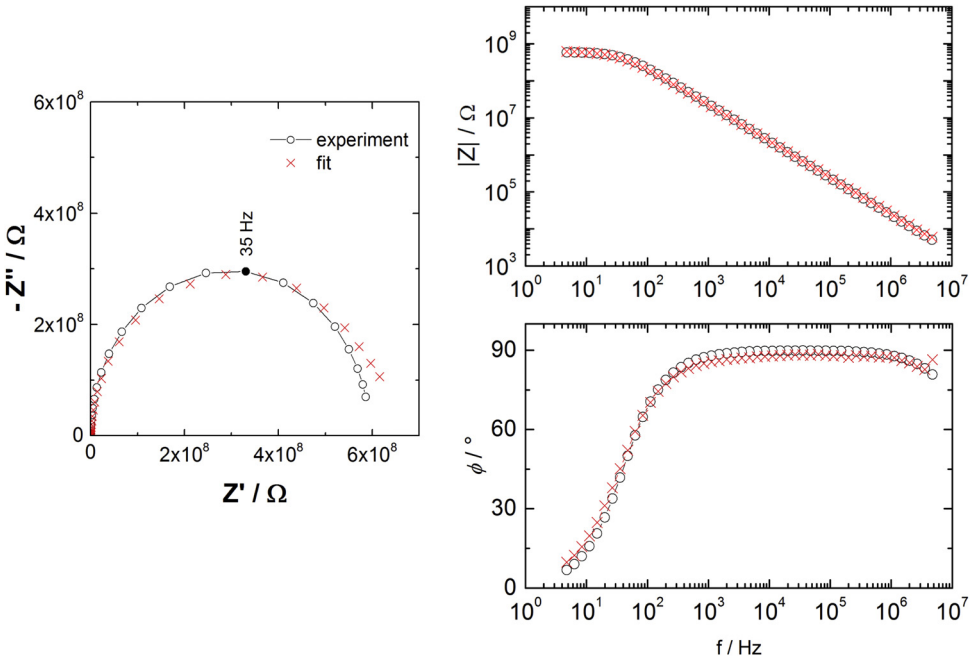

Fig. 6. Impedance diagram in Nyquist and Bode representation measured with a bi-microelectrode in air (open circles) and result of the fitting (red crosses) with a RC time constant (Voigt element) for the evaluation of the stray capacitance.

corresponding to the electrochemical contribution of the system corrected from the stray effect is obtained from

$$z_{loc} = z_{measured}\left(j\omega C_p 2\left(R_1 + \frac{R_2}{1 + j\omega R_2 C}\right) + 1\right) \quad (8)$$

Interestingly, in the low frequency domain ($\omega \to 0$), the local impedance is not influenced by the measuring device and

$$\lim_{\omega \to 0} z_{loc} = z_{measured} \quad (9)$$

whereas in the high frequency domain ($\omega \to \infty$), where the inductive behavior was observed for the local electrochemical impedance, the term $\frac{R_2}{1+j\omega R_2 C}$ tends towards 0 and the local impedance is thus expressed as

$$z_{loc} = z_{measured}(2j\omega R_1 C_p + 1) \quad (10)$$

This relation shows that the product $R_1 C_p$ is involved in the equation, meaning that without any independent determination of R_1 or C_p, one can only get the product of these two quantities from the fitting.

Fig. 7a shows the result of the local impedance fitting using Eq. 10 in combination with the Randles equivalent circuit for describing the electron exchange reaction in solution. A very good agreement with the experimental results is obtained. Moreover, the use of Eq. 10 allows correcting the impedance diagrams from the high frequency contribution, as shown in Fig. 7b. This local impedance diagram is very similar to the experimental result presented in Fig. 3 with a larger probe size, showing that it is possible to decrease the probe size, and thus to increase the spatial resolution for the LEIS measurement. Interestingly, a careful analysis of Eq. 10 shows that the corrective term that accounts for the stray capacitance multiplies the actual local impedance. In the high frequency domain, the local impedance response is dominated by the electrolyte resistance, thus the effect of the stray capacitance can be minimized by decreasing the electrolyte

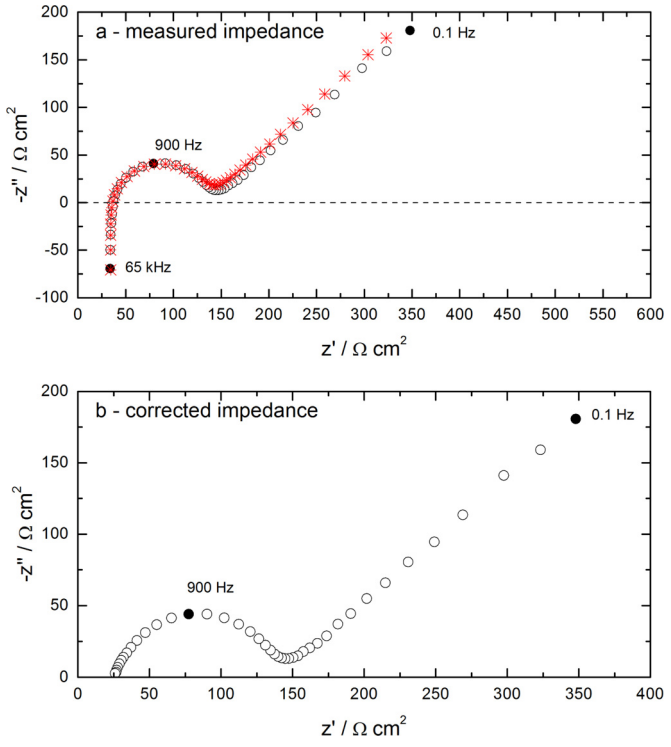

Fig. 7. Fit of the local impedance data using the Eq. 10 (a) and local impedance response corrected from the stray capacitance (b). Diameter of each wire: 20 μm; distance between wires: 15 μm; probe-to-sample distance h = 100 μm.

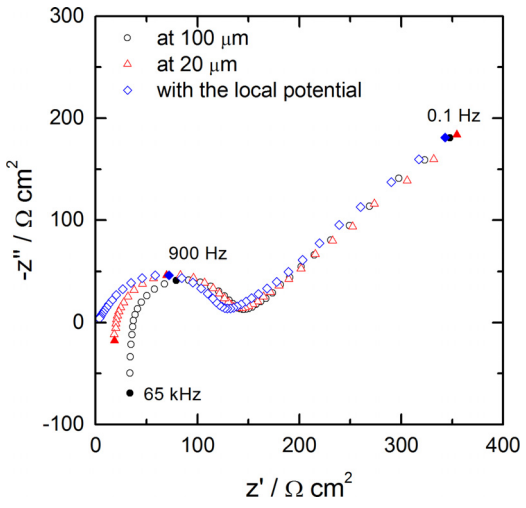

Fig. 8. Influence of the probe position on the HF behavior of the local impedance (black circles and red triangles) and the local interfacial impedance (blue diamonds). Diameter of each wire: 20 μm; distance between wires: 15 μm.

resistance, that is, by increasing the electrolyte conductivity or by decreasing the probe to sample distance.

Fig. 8 shows the influence of the probe-to-sample distance on the local impedance response, using the same probe. A significant effect can be seen in the high frequency behavior (black and red symbols). First, a shift towards higher electrolyte resistance value is observed as the distance increases, which is accompanied by an increase of the $R_1 C_p$ time-constant in this frequency domain. This is due to the fact that the uncompensated ohmic drop contribution increases with the distance. In order to decrease this contribution, a possible solution is to measure both the local potential, and the local current density for the evaluation of the local interfacial impedance as previously performed in the literature [27,32]. In that case, the contribution of the electrolyte resistance is vanishingly small consistently with the short electrolyte path between the probe and the surface as shown in Fig. 8 (blue curve) and the local interfacial impedance result remains free from the stray capacitance contribution, even when the measurement was performed with a small probe. It should also be mentioned that the contribution of the electrolyte resistance is likely to depend on the particular location of the probe both in distance from the surface and along a radius of the electrode since it is determined by the local electrolyte resistivity and the current-potential field in the solution.

4. Conclusions

The local impedance spectroscopy can be performed using different probe sizes. When a small probe is used, *i.e.* in the range of few tens of micrometers or less, the high frequency domain shows an inductive behavior that was ascribed to the presence of a stray capacitance between the two wires forming the probe. It was also shown that LEIS diagrams can be easily corrected by a numerical post-treatment in as much as a preliminary characterization of the probe was made. From the modeling of the measuring device, it was shown that the time constant due to the combination of the stray capacitance and the electrolyte resistance is in the measurable domain, and the electrolyte resistance must be decreased in order to minimize the high-frequency contribution, in agreement with experimental results performed for different probe positions above the substrate. Moreover, this effect can also be minimized by measuring the local potential instead of the global one, that is, the local interfacial impedance. In that case, the ohmic contribution is

governed by the distance between the closest wire of the probe used for measuring the local current density and the substrate. The spatial resolution of the LEIS technique can thus be improved for reaching the micrometer scale using the local interfacial impedance to avoid the high frequency inductive behavior.

Acknowledgements

CAPES (BEX 7307/14-4) and COFECUB (Project Nº 806-14) are gratefully acknowledged for their financial support.

References

[1] G. Wittstock, Imaging localized reactivities of surfaces by scanning electrochemical microscopy, Topics in Applied Physics 85 (2003) 335–364.
[2] M.V. Mirkin, W. Nogala, J. Velmurugan, Y. Wang, Scanning electrochemical microscopy in the 21st century. Update 1: five years after, Phys. Chem. Chem. Phys. 13 (2011) 21196–21212.
[3] D. Polcari, P. Dauphin-Ducharme, J. Mauzeroll, Scanning Electrochemical Microscopy: A Comprehensive Review of Experimental Parameters from 1989 to 2015, Chemical Reviews 116 (2016) 13234–13278.
[4] K. Eckhard, W. Schuhmann, Alternating current techniques in scanning electrochemical microscopy (AC-SECM), Analyst 133 (2008) 1486–1497.
[5] A.S. Bandarenka, K. Eckhard, A. Maljusch, W. Schuhmann, Localized electrochemical impedance spectroscopy: visualization of spatial distributions of the key parameters describing solid/liquid interfaces, Anal Chem 85 (2013) 2443–2448.
[6] C. Gabrielli, F. Huet, M. Keddam, P. Rousseau, V. Vivier, Scanning Electrochemical Microscopy Imaging by Means of High-Frequency Impedance Measurements in Feedback Mode, J. Phys. Chem. B 108 (2004) 11620–11626.
[7] C. Gabrielli, E. Ostermann, H. Perrot, V. Vivier, L. Beitone, C. Mace, Concentration mapping around copper microelectrodes studied by scanning electrochemical microscopy, Electrochem. Commun. 7 (2005) 962–968.
[8] D. Trinh, M. Keddam, X.R. Novoa, V. Vivier, Alternating-Current Measurements in Scanning Electrochemical Microscopy, Part 1: Principle and Theory, ChemPhysChem 12 (2011) 2169–2176.
[9] D. Trinh, M. Keddam, X.R. Novoa, V. Vivier, Alternating Current Measurements in Scanning Electrochemical Microscopy, Part 2: Detection of Adsorbates, ChemPhysChem 12 (2011) 2177–2183.
[10] D. Trinh, M. Keddam, X.R. Nóvoa, V. Vivier, Characterization of adsorbates by transient measurements in Scanning Electrochemical Microscopy, Electrochim. Acta 131 (2014) 28–35.
[11] L.F. Jaffe, R. Nuccitelli, An ultrasensitive vibrating probe for measuring steady extracellular currents, J. Cell. Biol. 63 (1974) 614–628.
[12] H.S. Isaacs, The measurement of the galvanic corrosion of soldered copper using the scanning vibrating electrode technique, Corros. Sci. 28 (1988) 547–558.
[13] H.S. Isaacs, Initiation of stress corrosion cracking of sensitized type 304 stainless steel in dilute thiosulfate solution, J. Electrochem. Soc. 135 (1988) 2180–2183.
[14] R.S. Lillard, P.J. Moran, H.S. Isaacs, A novel method for generating quantitative local electrochemical impedance spectroscopy, J. Electrochem. Soc. 139 (1992) 1007–1012.
[15] F. Zou, D. Thierry, H.S. Isaacs, A high-resolution probe for localized electrochemical impedance spectroscopy measurements, J. Electrochem. Soc. 144 (1997) 1957–1965.
[16] V. Upadhyay, D. Battocchi, Localized electrochemical characterization of organic coatings: A brief review, Prog. Org. Coat. 99 (2016) 365–377.
[17] J.V. Nardeli, D.V. Snihirova, C.S. Fugivara, M.F. Montemor, E.R.P. Pinto, Y. Messaddecq, A.V. Benedetti, Localised corrosion assessement of crambe-oil-based polyurethane coatings applied on the ASTM 1200 aluminum alloy, Corros. Sci. 111 (2016) 422–435.
[18] E. Aragon, C. Merlatti, J.B. Jorcin, N. Pebere, Study of delamination of organic coatings by local electrochemical impedance spectroscopy, Eur.Fed.Corros. Publ. 45 (2007) 62–70.
[19] I. Annergren, D. Thierry, F. Zou, Localized electrochemical impedance spectroscopy for studying pitting corrosion on stainless steels, J. Electrochem. Soc. 144 (1997) 1208–1215.
[20] I. Annergren, F. Zou, D. Thierry, Application of localized electrochemical techniques to study kinetics of initiation and propagation during pit growth, Electrochim. Acta 44 (1999) 4383–4393.
[21] G. Galicia, N. Pebere, B. Tribollet, V. Vivier, Local and global electrochemical impedances applied to the corrosion behaviour of an AZ91 magnesium alloy, Corros. Sci. 51 (2009) 1789–1794.
[22] I. Frateur, V.M. Huang, M.E. Orazem, B. Tribollet, V. Vivier, Experimental Issues Associated with Measurement of Local Electrochemical Impedance, J. Electrochem. Soc. 154 (2007) C719–C727.
[23] I. Frateur, V.M.-W. Huang, M.E. Orazem, N. Pebere, B. Tribollet, V. Vivier, Local electrochemical impedance spectroscopy: Considerations about the cell geometry, Electrochim. Acta 53 (2008) 7386–7395.
[24] V.M.-W. Huang, V. Vivier, I. Frateur, M.E. Orazem, B. Tribollet, The global and local impedance response of a blocking disk electrode with local constant-phase-element behavior, J. Electrochem. Soc. 154 (2007) C89–C98.
[25] J.B. Jorcin, E. Aragon, C. Merlatti, N. Pebere, Delaminated areas beneath organic coating: A local electrochemical impedance approach, Corros. Sci. 48 (2006) 1779–1790.
[26] I. Frateur, E. Bayet, M. Keddam, B. Tribollet, Local redox potential measurement, Electrochem. Commun. 1 (1999) 336–340.
[27] V.M.-W. Huang, S.-L. Wu, M.E. Orazem, N. Pebere, B. Tribollet, V. Vivier, Local electrochemical impedance spectroscopy: A review and some recent developments, Electrochim. Acta 56 (2011) 8048–8057.
[28] E. Bayet, F. Huet, M. Keddam, K. Ogle, H. Takenouti, A novel way of measuring local electrochemical impedance using a single vibrating probe, J. Electrochem. Soc. 144 (1997) L87–L90.
[29] J.V. Ferrari, H.G. de Melo, M. Keddam, M.E. Orazem, N. Pebere, B. Tribollet, V. Vivier, Influence of normal and radial contributions of local current density on local electrochemical impedance spectroscopy, Electrochim. Acta 60 (2012) 244–252.
[30] G. Baril, C. Blanc, M. Keddam, N. Pebere, Local electrochemical impedance spectroscopy applied to the corrosion behavior of an AZ91 magnesium alloy, J. Electrochem. Soc. 150 (2003) B488–B493.
[31] N. Pébère, V. Vivier, Local Electrochemical Measurements in Bipolar Experiments for Corrosion Studies, ChemElectroChem 3 (2016) 415–421.
[32] E. Bayet, F. Huet, M. Keddam, K. Ogle, H. Takenouti, Local electrochemical impedance measurement: scanning vibrating electrode technique in ac mode, Electrochim. Acta 44 (1999) 4117–4127.
[33] R. Sihlbom, M. Dernevik, M. Lindgren, J.P. Starski, Z. Lai, J. Liu, High frequency measurements and simulations on wire-bonded modules on the sequential build-up boards (SBU's), IEEE Transactions on Components Packaging and Manufacturing Technology Part A 21 (1998) 478–491.